# Improvement of doping efficiency in Mg-$Al_{0.14}Ga_{0.86}N$/GaN superlattices with AlN interlayer by suppressing donor-like defects*

Liu Ning-Yang(刘宁炀), Liu Lei(刘 磊), Wang Lei(王 磊), Yang Wei(杨 薇), Li Ding(李 丁), Li Lei(李 磊), Cao Wen-Yu(曹文彧), Lu Ci-Mang(鲁辞莽), Wan Cheng-Hao(万成昊), Chen Wei-Hua(陈伟华), and Hu Xiao-Dong(胡晓东)†

*State Key Laboratory for Artificial Microstructure and Mesoscopic Physics, School of Physics, Peking University, Beijing* 100871, *China*

(Received 5 April 2012; revised manuscript received 3 July 2012)

We investigate the mechanism for the improvement of p-type doping efficiency in Mg-$Al_{0.14}Ga_{0.86}N$/GaN superlattices (SLs). It is shown that the hole concentration of SLs increases by nearly an order of magnitude, from $1.1\times10^{17}$ to $9.3\times10^{17}$ cm$^{-3}$, when an AlN interlayer is inserted to modulate the strains. Schrödinger–Poisson self-consistent calculations suggest that such an increase could be attributed to the reduction of donor-like defects caused by the strain modulation induced by the AlN interlayer. Additionally, the donor-acceptor pair emission exhibits a remarkable decrease in intensity of the cathodoluminescence spectrum for SLs with an AlN interlayer. This supports the theoretical calculations and indicates that the strain modulation of SLs could be beneficial to the donor-like defect suppression as well as the p-type doping efficiency improvement.

**Keywords:** superlattice, doping efficiency, strain modulation, nitrogen vacancy

**PACS:** 73.21.Cd, 71.55.Eq, 78.66.Fd **DOI:** 10.1088/1674-1056/21/11/117304

## 1. Introduction

The development of high p-type doping efficiency is crucial to the performance of GaN-based electronic and optoelectronic devices. Since the discovery of p-type conductivity in magnesium (Mg) doped GaN by low-energy electron irradiation[1] and thermal annealing method,[2] remarkable achievements have been made in the area of solid-state lighting. Current high-brightness GaN-based light-emitting diodes as well as laser diodes are commercially available and widely used. However, it is notable that the hole concentration is typically low for most of the GaN-based materials that use the metalorganic vapor phase epitaxial (MOVPE) system. The low hole concentrations are typically from $10^{17}$ to $5\times10^{17}$ cm$^{-3}$ due to the large acceptor activation energy ($E_a$) and the strong self-compensation effect of native defects. Early work suggested an energy of at least 150 meV for Mg activation in GaN, and higher in $Al_xGa_{1-x}N$ with increasing Aluminum content.[3] To overcome the obstacle, $Al_xGa_{1-x}N$/GaN SLs structure has been proposed and demonstrated to have lower activation energy than bulk GaN or $Al_xGa_{1-x}N$.[4,5] Meantime, the compensation of acceptors mainly comes from a substantial amount of nitrogen vacancies ($V_N$) which have very low formation energy in heavily Mg-doped AlGaN alloys.[6] Therefore, an appropriate doping level of Mg ($1\times10^{19}$–$2\times10^{19}$ cm$^{-3}$) was proposed to minimize the compensation effect.[7] It has recently been reported that strain modulation severely affects the equivalent activation energy of Mg in SLs.[8] This means that, with an AlN interlayer inserted before the growth of $Al_xGa_{1-x}N$/GaN SLs, the $Al_xGa_{1-x}N$ barrier layers will contain less tensile strains, while the GaN well layers will suffer a little more compressive strains, leading to the decrease of the equivalent activation energy from 150 to 70 meV. Despite this breakthrough, further analysis is required to explore the reason for the hole-concentration enhancement re-

*Project supported by the National Natural Science Foundation of China (Grant Nos. 61076012, 61076013, and 51102003), the National High Technology Research and Development Program of China (Grant No. 2007AA03Z403), the Specialized Research Fund for the Doctoral Program of Higher Education, China (Grant No. 20100001120014), and the National Basic Research Program of China (Grant No. 2012CB619304).

†Corresponding author. E-mail: huxd@pku.edu.cn

© 2012 Chinese Physical Society and IOP Publishing Ltd

sulting from strain modulation. Future studies on this mechanism would appear to be interesting.

In this work, the influence of strain modulation induced by AlN interlayer on hole-concentration enhancement of SLs is confirmed again. The classical Schrödinger–Poisson self-consistent solver is introduced to investigate the mechanism behind the improved p-type doping efficiency. Cathodoluminescence (CL) spectrum measurements are performed to support the calculation findings. The relationship between the strain modulation and donor-like defect suppression and hence the improved p-type doping efficiency is disclosed.

## 2. Experimental methods

SLs samples used in this study were deposited in a Thomas Swan MOVPE system. Trimethlgallium, trimethylaluminum, and ammonia were used as the precursors for Ga, Al, and N sources, respectively. After deposition of 30-nm buffer layer on a sapphire substrate, a 3-μm unintentionally doped GaN was grown, followed by a 600-nm SLs structure at 1099 °C with or without an AlN interlayer. Sample A without an AlN interlayer was first grown, which consists of GaN wells and $Al_{0.14}Ga_{0.86}N$ barriers (3 nm/3 nm, ×100 periods). Then a 10-nm AlN interlayer at the same growth temperature as SLs was introduced between the undoped GaN and SLs for sample B (3 nm/3 nm, ×100 periods). Another three samples with AlN interlayer were grown for comparison, which consist of ×200 periods (1.6 nm/1.6 nm), ×50 periods (5.9 nm/5.9 nm), and ×34 periods (8.8 nm/8.8 nm), respectively. All samples were uniformly Mg-doped ($N_{Mg} \approx 10^{19}$ cm$^{-3}$), and annealed at 800 °C in $N_2$ ambient for 15 min for Mg activation.

High-resolution X-ray diffraction (HR-XRD) $\omega$–$2\theta$ scans and $\omega$ scans were conducted on the samples to investigate the structural parameters and threading dislocations (TDs). Room-temperature Hall-effect measurements were performed using the van der Pauw geometry to obtain hole concentrations. The CL spectra were obtained at 81 and 300 K under the condition of 25 kV and 300 pA using Gatan MonoCL3 plus equipment installed in a scanning electron microscope.

## 3. Results and discussion

Figure 1 shows the HR-XRD (002)-plane and (104)-plane $\omega$–$2\theta$ scans of samples A and B. The GaN peaks mainly come from the undoped GaN layers, and have the same angle for samples A and B. It is interesting to note that the zero-order SLs peak of sample B shifts to a lower angle compared with that of sample A, which is probably due to less Al content or more compressive strains in sample B. Moreover, there is a broad AlN peak in the scan curve of sample B, indicating the existence of an AlN interlayer. No counterpart can be seen for sample A.

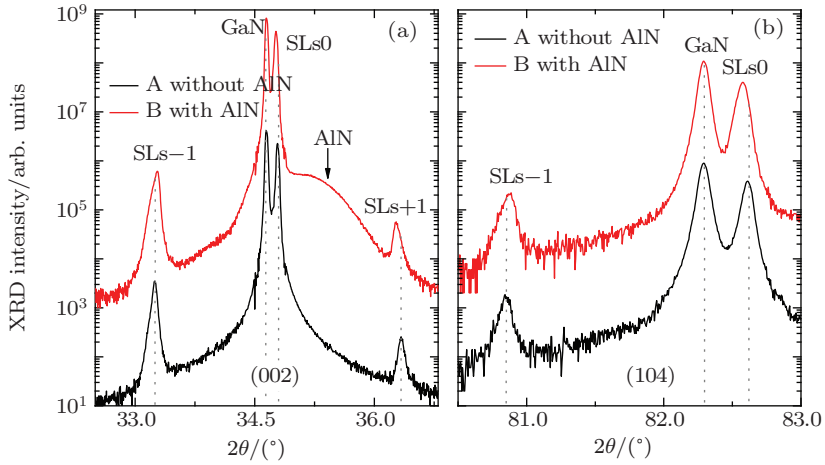



**Fig. 1.** (colour online) (a) HR-XRD (002)-plane and (b) (104)-plane $\omega$–$2\theta$ scan curves for Mg-doped $Al_{0.14}Ga_{0.86}N$/GaN SLs with and without an AlN interlayer.

The in-plane lattice constant $a$ and out-plane lattice constant $c$ are first obtained and listed in Table 1. Then the Al contents are set to 14.30% for sample A and 13.68% for sample B, using the approach described in Ref. [9]. These results are almost consistent with our growth design. The periods are deduced

from satellite peaks, which are 6.0 nm for sample A and 6.2 nm for sample B. The biaxial strain in the GaN well or $Al_xGa_{1-x}N$ barrier layers can be determined by[10]

$$\varepsilon_j = (a_{\rm SLs} - a_j)/a_j, \quad (1)$$

where $a_{\rm SLs}$ is the measured lattice parameter for SLs, and $a_j$ (predicted by Vegard's law) is the totally relaxed lattice parameter for GaN well ($Al_xGa_{1-x}N$ barrier) layers. It turns out that for sample A without AlN interlayer, the GaN well layers are free of strains, while the $Al_xGa_{1-x}N$ barrier layers are expanded (the residual strain in barrier layers $\varepsilon_{\rm barriers}$ is positive). For sample B with an AlN interlayer, however, the GaN well layers are compressed (the residual strain in well layers $\varepsilon_{\rm wells}$ is negative), while the $Al_xGa_{1-x}N$ barrier layers are less expanded. This means that the AlN interlayer can effectively modulate the strain distribution between GaN wells and $Al_xGa_{1-x}N$ barriers in SLs.

**Table 1.** Structural and compositional parameters of SLs obtained from HR-XRD measurement. The biaxial strains and the resulting variations in energy band edge were also listed.

| Samples | $a_{\rm GaN}$/Å | $c_{\rm GaN}$/Å | $a_{\rm SLs}$/Å | $c_{\rm SLs}$/Å | Period/nm | Al content/% | $\varepsilon_{\rm wells}$ | $dE_{\rm wells}$/eV | $\varepsilon_{\rm barriers}$ | $dE_{\rm barriers}$/eV |
|---|---|---|---|---|---|---|---|---|---|---|
| A | 3.185 | 5.185 | 3.185 | 5.164 | 6.0 | 14.30% | 0 | 0 | 0.00317 | –0.0318 |
| B | 3.185 | 5.185 | 3.183 | 5.167 | 6.2 | 13.68% | –0.00063 | 0.0061 | 0.00291 | –0.0249 |

In order to investigate the influence of strain modulation on the electric properties of SLs, Hall-effect measurements were performed at 300 K. The measured hole concentration shows a nearly tenfold enhancement from sample A to B, which is from $1.1\times10^{17}$ to $9.3\times10^{17}$ cm$^{-3}$. To understand the relation between the hole concentration enhancement and the strain modulation of SLs, an in-depth analysis is carried out and presented below.

The doping characteristics of Mg-$Al_xGa_{1-x}N$/GaN SLs were investigated theoretically using a classical Schrödinger–Poisson self-consistent solver.[11] In the calculations, the equilibrium Fermi level was fixed at 0 eV, and the Al contents were $x = 14.3\%$ for sample A and $x = 13.7\%$ for sample B, respectively. The energy band gap ($E_{\rm g}$) of relaxed GaN at 300 K was chosen as 3.402 eV, AlN 6.158 eV, and $Al_{0.14}Ga_{0.86}N$ 3.704 eV with a bowing parameter 0.7. The band-offset ratio used here was 0.67:0.33. The influence of biaxial strains on the energy band edge was also considered. According to previous research,[12] the variations in band edge ($dE$) and biaxial strain ($d\varepsilon$) are connected through the deformation potential $dE/d\varepsilon$, which are $-9.71$ eV for GaN and $-8.57$ eV for $Al_{0.14}Ga_{0.86}N$, respectively. Given the biaxial strains obtained from HR-XRD, the band gaps and band offsets in SLs were renewed. It was shown that for sample A, the $E_{\rm g}$ of GaN and $Al_xGa_{1-x}N$ remains 3.402 eV and 3.672 eV, respectively, and the resulting conduction-band discontinuity ($\Delta E_{\rm c}$) was 181 meV; while for sample B, the $E_{\rm g}$ of GaN and $Al_xGa_{1-x}N$ increases to 3.408 eV and 3.679 eV, respectively, and the $\Delta E_{\rm c}$ was 182 meV. Thus, the energy band edge and band offset were found to be insensitive to the distinction between samples A and B. Another important effect of the strains is to change the piezoelectric component of polarization. The piezoelectric polarization ($P^{\rm PZ}$) of SLs are given by[13]

$$\begin{aligned} &P^{\rm PZ}_{\rm AlN} = -1.808\varepsilon - 7.888\varepsilon^2, \quad (\varepsilon > 0),\\ &P^{\rm PZ}_{\rm GaN} = -0.918\varepsilon + 9.541\varepsilon^2,\\ &P^{\rm PZ}_{\rm AlGaN}(x) = xP^{\rm PZ}_{\rm AlN}(\varepsilon(x)) + (1-x)P^{\rm PZ}_{\rm GaN}(\varepsilon(x)). \end{aligned} \quad (2)$$

Then, the total polarization ($P$) is

$$P = P^{\rm SP} + P^{\rm PZ}, \quad (3)$$

where $P^{\rm SP}$ is the spontaneous polarization of GaN well or $Al_xGa_{1-x}N$ barrier layers. The total polarization is calculated to be $3.40\times10^{-6}$ C/cm$^2$ for GaN wells and $4.70\times10^{-6}$ C/cm$^2$ for $Al_xGa_{1-x}N$ barriers in sample A. In sample B, the values were $3.34\times10^{-6}$ C/cm$^2$ for wells and $4.58\times10^{-6}$ C/cm$^2$ for barriers, respectively. The differences in polarization would affect the periodic potential of SLs, and consequently the hole carrier distributions. In addition, it can be expected that the biaxial strains have impacts on the level of Mg acceptors ($N_{\rm a}$) incorporated in SLs, the activation energy ($E_{\rm a}$) of Mg, or the amount of native donor-like defects ($N_{\rm d}$) generated during the growth process. Because the correlation between biaxial strains and $N_{\rm a}$ is not clear, the $N_{\rm a}$ should be considered as a variable parameter, which is in a range of $3\times10^{17}$–$1\times10^{19}$ cm$^{-3}$

in our calculations. The same considerations were taken for $E_a$ and $N_d$. The activation energy of Mg in GaN ranges from 170 to 340 meV, and in $Al_xGa_{1-x}N$ it is determined by[14]

$$E_a\,[\mathrm{AlGaN}\,(x)] = E_a\,(\mathrm{GaN}) + 437.5x. \qquad (4)$$

The donor-like defects have a level range of $N_d = 0$–$5.2\times10^{18}$ cm$^{-3}$, and they are assumed to be fully ionized. The other parameters are carefully set to the same values as in Ref. [15].

In general, the energy band diagram of SLs can be first obtained after running the Schrödinger–Poisson self-consistent solver. Then, the hole carrier distribution ($p$) and the energy band diagram are related as follows:[16]

$$p = N_v \exp\left[-(E_F - E_v)/k_BT\right], \qquad (5)$$

where $N_v$ is the equivalent state density of the valence band, $E_F$ Fermi level, $E$v valence band, and $k_B$ Boltzmann constant. Finally, the hole concentration of SLs can be determined by averaging the hole carrier distribution. Therefore, a set of parameters corresponds to one energy band diagram, and hence one spatially averaged hole concentration of SLs. Some interesting results are obtained when taking into account various sets of parameters, which are shown below.

Figure 2 shows the spatially averaged hole concentration of SLs as a function of $N_a$, $E_a$, and $N_d$, respectively. It turns out that the acceptor's doping level, activation energy, and the amount of donor-like defects can be expected to be significant influential factors of p-type doping efficiency in SLs. Therefore, the enhancement of hole concentration is probably due to an increase of $N_a$ ($> 4\times10^{18}$ cm$^{-3}$), a dramatic reduction of $E_a$ ($> 100$ meV), or a decrease of $N_d$ ($> 3\times10^{18}$ cm$^{-3}$) from sample A to B.

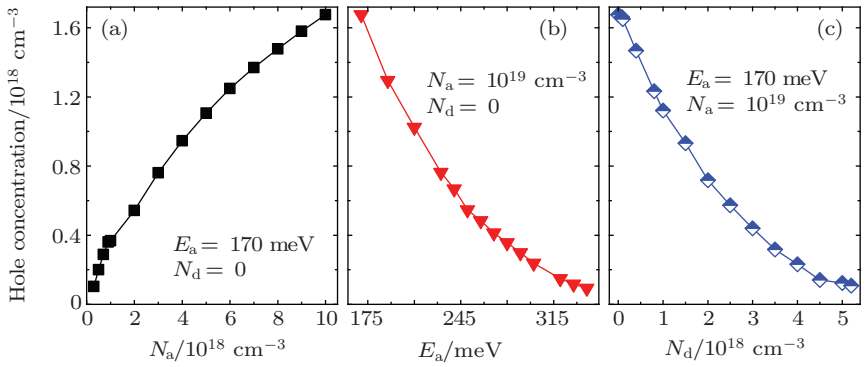



**Fig. 2.** (colour online) Spatially averaged hole concentration of SLs as a function of (a) acceptor's doping level, (b) acceptor activation energy, and (c) the amount of donor-like defects.

Take $N_d$ for example, the band diagrams of SLs are plotted in Fig. 3 when $N_d = 5.0\times10^{18}$ cm$^{-3}$ for sample A and $N_d = 1.4\times10^{18}$ cm$^{-3}$ for sample B. The resulting spatially averaged hole concentrations are $1.20\times10^{17}$ and $9.41\times10^{17}$ cm$^{-3}$ for samples A and B, respectively, which are in very close agreement with the experimental data.

In order to further confirm the main factor causing the improvement of the p-type doping efficiency and to understand the origin of donor-like defects, the CL spectrum measurements were performed at 300 and 81 K. Two peaks were detected in the wavelength range of 320–520 nm at 300 K, as shown in the inset of Fig. 4. A remarkable decrease in the intensity of the DAP emission can be seen by comparing sample A with B. Specifically, Peak I at 350 nm with a narrow full width at half maximum (FWHM) of 8 nm is attributed to the CL emission of sub-bands in SLs. By contrast, Peak II at 409 nm has a broad FWHM and is expected to be a donor-acceptor pair (DAP) emission, which is the characteristic recombination process in Mg-doped GaN or AlGaN alloys. The transition associated with DAP is from deep donors to shallow acceptors, where the donors are suggested to be nitrogen vacancies ($V_N$) in Ref. [17]. Due to the suppression of phonons, more peaks and optical fringes are visible in the CL spectra at 81 K. Peak I splits into Peaks 1 and 2, as shown in Fig. 4. Peak 3 (362.2 nm) and Peak 4 (374.5 nm) are considered as CL emissions from another sub-band in SLs. The Peaks 3 and 4 were too weak to be distinguished in the spectrum of sample B, which is probably because the overlaps

of electron and hole wave functions are small in those sub-bands.[18] The DAP peak emissions are around 380 nm and worth detailed discussion as follows.

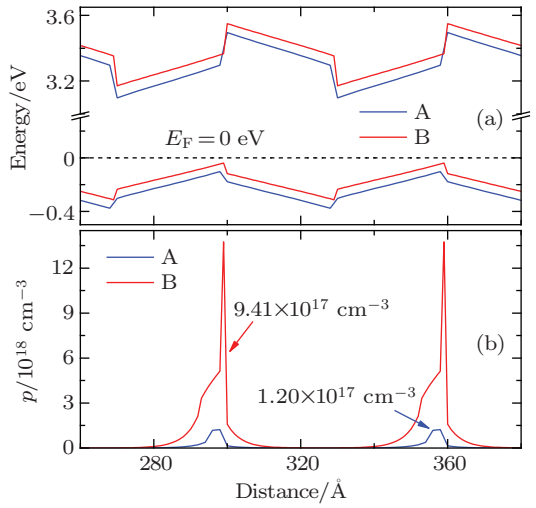



**Fig. 3.** (colour online) (a) Simulated energy-band diagrams and (b) hole distribution in SLs sample A with $N_d = 5.0 \times 10^{18}$ cm$^{-3}$ and sample B with $N_d = 1.4 \times 10^{18}$ cm$^{-3}$, respectively.

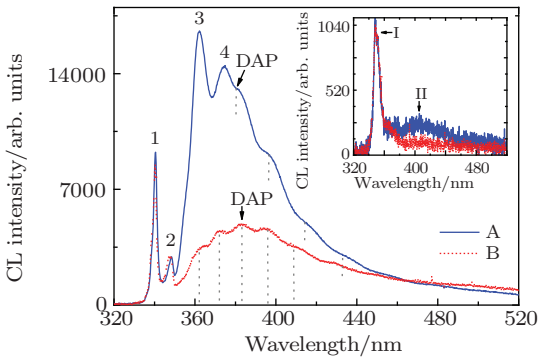



**Fig. 4.** (colour online) CL spectra for SLs obtained at 300 K (inset) and 81 K. The characteristic peaks are labelled by numbers or "DAP". The optical fringes are shown by grey dotted lines.

First, the DAP peak red-shifts a little from samples A (380.2 nm) to B (383.5 nm). This corresponds to a 28-meV shift in energy and is likely due to the increase of $E_a$ of donors or acceptors in sample B. Therefore, the assumed dramatic decrease of $E_a$ for sample B in the calculation is logically impossible. Second, the arbitrary intensity of the DAP peak decreases by a factor of 2.8 from samples A to B. The intensity of DAP emission depends on the amounts of $N_a$ and $N_d$. Especially the amount of $N_d$ should be dominant in this situation since donor-like defects are the minority in p-type materials. Thus, the result implies a significant reduction of the amount of $N_d$. Far more likely, it is the reduction of $N_d$ that results in the improvement of p-type doping efficiency. The donors within p-type SLs are presumably nitrogen vacancies ($V_N$) as aforementioned. Finally, the center of the energy level of $V_N$ is deduced to be 200 meV below the conduction band minimum, given that the GaN band gap is 3.402 eV and $E_a$ 170 meV. This value is of the same order of magnitude as the previous result of 150±20 meV reported by deep-level transient spectroscopy spectra.[19]

We have additional evidences from XRD rocking curves (RCs) and Hall-effect measurements that help us further understand the mechanism behind the improvement of p-type doping efficiency. Figure 5 shows the RCs of SLs in (002)-plane and (104)-plane. Compared with that of sample A, the peak center of sample B shifts to a lower angle due to less Al contents and more compressive strains in SLs. It is interesting to note that in each plane the FWHM of RC in sample B is larger than that in sample A, indicating an increase of TDs resulting from the insert of an AlN interlayer.

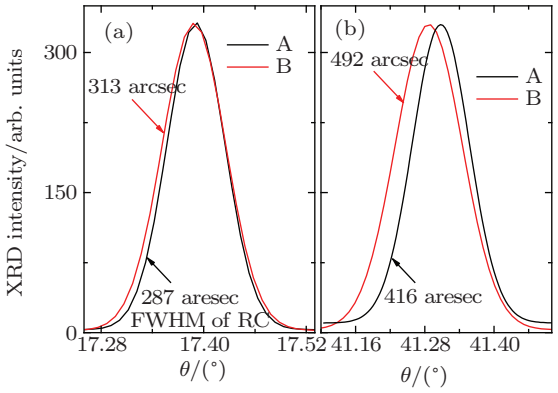



**Fig. 5.** (colour online) Rocking curves of samples A and B in (a) (002)-plane and (b) (104)-plane $\omega$ scans. Each scan shows an increase of FWHM from sample A to B.

Moreover, Hall-effect measurements were performed for the other three samples with periods of 3.2, 11.8, and 17.6 nm. The Schrödinger–Poisson self-consistent solver was also run for SLs with various periods (from 3 to 18 nm) for comparison. A good match between the theoretical prediction and experimental data is obtained, as shown in Fig. 6. The calculations suggest that the values of $N_d$ are around $7.0\times10^{17}$, $1.4\times10^{18}$, $2.0\times10^{18}$, and $2.1\times10^{18}$ cm$^{-3}$ for the SLs with periods of 3, 6, 12, and 18 nm, respectively. This implies a small increase in $V_N$ with increasing periods.

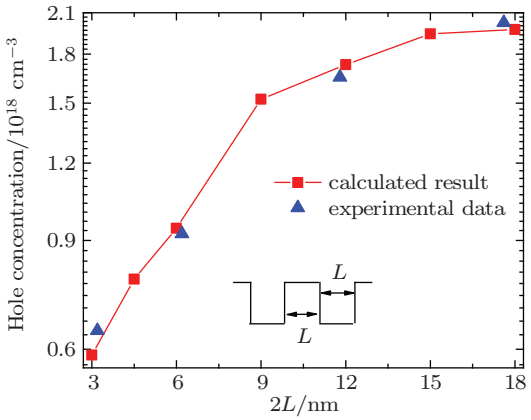



**Fig. 6.** (colour online) Comparison of theoretical predictions of the hole concentration with experimental observations for SLs. The period ($2L$) increases from 3 to 18 nm.

Based on these results, a possible mechanism is speculated as follows. 1) The AlN interlayer increases the compressive strains in GaN well layers and reduces the tensile strains in the $Al_xGa_{1-x}N$ barrier layers. Thus, the whole SLs are under less tensile strain, leading to the suppression of $V_N$ and the enhancement of hole concentration. 2) The relaxations of the strains in the GaN well layers will increase the TDs, causing the broadening of FWHM in RCs. 3) When the thickness of GaN wells is small, i.e., 3.1 nm in sample B, the relaxation process is not exhaustive. When the periods increase, however, the strain relaxation in the GaN well layers also increases and the consequent strain modulation in the $Al_xGa_{1-x}N$ barrier layers becomes less effective, causing the relative increase of $V_N$. Finally, we can draw a conclusion that the strain modulation induced by the AlN interlayer can suppress the donor-like defects ($V_N$) in Mg-doped $Al_xGa_{1-x}N$/GaN SLs, and hence improve the p-type doping efficiency dramatically. It seems that less tensile strains or more compressive strains are beneficial to the suppression of $V_N$, which requires more direct experimental evidences.

## 4. Conclusion

In summary, we have investigated the p-type doping efficiency in Mg-$Al_{0.14}Ga_{0.86}N$/GaN SLs with or without a 10-nm AlN interlayer. The measured hole concentration of SLs increases from $1.1\times10^{17}$ to $9.3\times10^{17}$ cm$^{-3}$ due to the insert of AlN interlayer. By combining the Schrödinger–Poisson self-consistent calculation results and the CL spectrum analysis, it can be deduced that the strain modulation of SLs effectively suppresses the donor-like defects ($V_N$), and consequently enhances the p-type doping efficiency. Thus, both the GaN materials and the device performance can be improved.

## Acknowledgements

The authors would like to thank the staff at the beam-line 1W1A at the Beijing synchrotron radiation facility for the HR-XRD measurements.

## References

[1] Akasaki I, Amano H, Kito M and Hiramatsu K 1991 *J. Lumin.* **48** 666
[2] Nakamura S, Mukai T, Senoh M and Iwasa N 1992 *Jpn. J. Appl. Phys.* **31** L139
[3] Jain S C, Willander M, Narayan J and Van Overstraeten R 2000 *J. Appl. Phys.* **87** 965
[4] Schubert E F, Grieshaber W and Goepfert I D 1996 *Appl. Phys. Lett.* **69** 3737
[5] Kozodoy P, Hansen M, DenBaars S P and Mishra U K 1999 *Appl. Phys. Lett.* **74** 3681
[6] Stampfl C and Van de Walle C G 2002 *Phys. Rev.* B **65** 155212
[7] Kaufmann U, Schlotter P, Obloh H, Köhler K and Maier M 2000 *Phys. Rev.* B **62** 10867
[8] Wang L, Li R, Li D, Liu N Y, Liu L, Chen W H, Wang C D, Yang Z J and Hu X D 2010 *Appl. Phys. Lett.* **96** 061110
[9] Pereira S, Correia M R, Pereira E, O'Donnell K P, Martin R W, White M E, Alves E, Sequeira A D and Franco N 2002 *Mater. Sci. Eng.* B **93** 163
[10] Guo X, Wang Y T, Zhao D G, Jiang D S, Zhu J J, Liu Z S, Wang H, Zhang S M, Qiu Y X, Xu K and Yang H 2010 *Chin. Phys.* B **19** 076804
[11] Snider G 2005 *1D Poisson–Schrödinger Solver* (Department of Electrical Engineering, University of Notre Dame) available at http://www.nd.edu/∼gsnider/
[12] Ridley B K, Schaff W J and Eastman L F 2003 *J. Appl. Phys.* **94** 3972
[13] Ambacher O, Majewski J, Miskys C, Link A, Hermann M, Eickhoff M, Stutzmann M, Bernadini F, Fiorentini V, Tilak V, Schaff B and Eastman L F 2002 *J. Phys.: Condens. Matter* **14** 3399
[14] Tanaka T, Watanabe A, Amano H, Kobayashi Y, Akasaki I, Yamazaki S and Koike M 1994 *Appl. Phys. Lett.* **65** 593
[15] Vurgaftman I and Meyer J R 2003 *J. Appl. Phys.* **94** 3675
[16] Sze S M and Ng K K 2007 *Physics of Semiconductor Devices* (3rd edn.) (Hoboken: John Wiley & Sons) p. 19
[17] Song J J and Shan W 1998 *Group III Nitride Semiconductor Compounds: Physics and Applications* (edited by Gill B) (Oxford: Clarendon) p. 182
[18] Cai D J and Guo G Y 2010 *J. Appl. Phys.* **107** 103533
[19] Hogsed M R, Yeo Y K, Ahoujja M, Ryu M Y, Petrosky J C and Hengehold R L 2005 *Appl. Phys. Lett.* **86** 261906